Bioreplicated visual features of nanofabricated buprestid beetle decoys evoke stereotypical male mating flights

Michael J. Domingue[a,1], Akhlesh Lakhtakia[b], Drew P. Pulsifer[b], Loyal P. Hall[a], John V. Badding[c], Jesse L. Bischof[c], Raúl J. Martín-Palma[d], Zoltán Imrei[e], Gergely Janik[f], Victor C. Mastro[g], Missy Hazen[h], and Thomas C. Baker[a,1]

Departments of [a]Entomology, [b]Engineering Science and Mechanics, [c]Chemistry, and [d]Materials Science and Engineering, Pennsylvania State University, University Park, PA 16802; [e]Plant Protection Institute, Centre for Agricultural Research, Hungarian Academy of Sciences, H-3232 Budapest, Hungary; [f]Department of Forest Protection, Forest Research Institute, H-1022 Mátrafüred, Hungary; [g]Animal and Plant Health Inspection Service, Plant Protection and Quarantine, Center for Plant Health Science and Technology, US Department of Agriculture, Buzzards Bay, MA 02542; and [h]Huck Institutes of the Life Sciences Microscope Facilities, Pennsylvania State University, University Park, PA 16802

Recent advances in nanoscale bioreplication processes present the potential for novel basic and applied research into organismal behavioral processes. Insect behavior potentially could be affected by physical features existing at the nanoscale level. We used nano-bioreplicated visual decoys of female emerald ash borer beetles (*Agrilus planipennis*) to evoke stereotypical mate-finding behavior, whereby males fly to and alight on the decoys as they would on real females. Using an industrially scalable nanomolding process, we replicated and evaluated the importance of two features of the outer cuticular surface of the beetle's wings: structural interference coloration of the elytra by multilayering of the epicuticle and fine-scale surface features consisting of spicules and spines that scatter light into intense strands. Two types of decoys that lacked one or both of these elements were fabricated, one type nano-bioreplicated and the other 3D-printed with no bioreplicated surface nanostructural elements. Both types were colored with green paint. The light-scattering properties of the nano-bioreplicated surfaces were verified by shining a white laser on the decoys in a dark room and projecting the scattering pattern onto a white surface. Regardless of the coloration mechanism, the nano-bioreplicated decoys evoked the complete attraction and landing sequence of *Agrilus* males. In contrast, males made brief flying approaches toward the decoys without nanostructured features, but diverted away before alighting on them. The nano-bioreplicated decoys were also electroconductive, a feature used on traps such that beetles alighting onto them were stunned, killed, and collected.

nanofabrication | structural color | spectral emission | visual response | supercontinuum laser

Biomimicry of insect visual communication signals has received much recent attention, with growing interest in nanofabrication processes that result in artificially produced structural colors (1) such as those emanating from the ridges on butterfly wing scales (2). The fidelity of the nanoreplication of visual signals with communication value to such organisms has been underexplored, however. Visually induced behavior in arthropods often integrates color and edge-motion detection, with interactions often involving a variety of biotic and abiotic entities, making it difficult to reproduce experimentally (3).

Bioreplication of visual signaling structures might be manipulated so as to provide insight into the mechanisms of such signaling processes; however, all currently known examples of bioreplicated nanostructures that have been created to affect behavior involve unicellular movements across particular textured environments (4–7), rather than directed to evoke responses of specialized sensory organs of more complex multicellular organisms. Bioreplicated structures emitting behaviorally effective visual cues also may be useful for such practical purposes as the monitoring

and detection of pest species, but the communication efficacy of the bioreplica needs to be validated under field conditions using naturally occurring (i.e., wild) populations.

In contrast, biomimicry of chemical signals, such as insect pheromones, has been a burgeoning field for more than half a century. Synthetically reproduced pheromones have been successfully applied under field conditions to manipulate insect behavior for invasive species pest detection, population monitoring of endemic species, and disruption of mating. Thousands of studies have described the essential components of nanoscale levels (nanograms) of semiochemical signals that trigger behavioral responses, such as upwind flight for mating (8), alarm responses (9), and trail following (10). Furthermore, neurophysiological techniques have elucidated how these signals are transduced by peripheral sensory organs (11) and integrated into odor sensations in the higher processing centers of the insect brain (12). In the realm of applied science, these insights have led to trapping protocols for pest population detection, attract-and-kill protocols, and mating disruption (13). Visually attractive features of trapping technologies generally have not been approached with such rigor, however, and are usually optimized by simple manipulations of trap colors without efforts to understand the underlying mechanisms of visual attraction.

In an effort to initiate such an approach to manipulation of visual signaling systems, we used an industrially scalable nano-bioreplication technique (14) to produce high-fidelity replicas of

APPLIED BIOLOGICAL SCIENCES

the structural features of the cuticle of the hard wing covers (elytra) of an invasive buprestid beetle pest, the emerald ash borer (*Agrilus planipennis*). This species is a tree-killing pest of Asian origin whose visual signal is emitted by the elytra of a female at rest on an ash leaf in direct sunlight, which triggers attraction of flying males that are patrolling the canopy. Male responses unfold as rapid flights toward the females from heights of up to 2 m, usually terminating with the males alighting directly on the females and attempting to copulate (15). This "paratrooper" descent behavior by flying *A. planipennis* males in the field can be repeatedly evoked by affixing dead *A. planipennis* females to ash leaves (15, 16). Furthermore, various other potentially invasive European and North American tree-feeding *Agrilus* species have been observed performing similar stereotypical inflight descents onto dead beetle decoys affixed to the leaves of preferred host trees (17, 18). Such approaches are often seen to congeneric, heterospecific targets. One such species, the two-spotted oak borer, *Agrilus biguttatus*, that is similar in size and habits to *A. planipennis* is known to kill oak trees within its native range in Europe (19), particularly after drought (20) or defoliation events (21).

The base colors of many metallic-colored beetles, including buprestid beetles (Fig. 1*A*), are known to be structurally produced by the repeated alternation of cuticle layers (Fig. 1*D*) with different refractive indices (22, 23). This periodically multilayered assemblage functions as a quarter-wave Bragg stack reflector in a particular spectral regime (2) and is thus highly effective for creating a color of narrow specificity in sunlight, unlike many naturally occurring pigments. The reflected light is also affected by regular fine-scale topographic features of the surface, including thousands of sharp spicules each emitting green to yellow colors, which are further scattered by numerous spines (Fig. 1 *B* and *C*). Many of the physical attributes of the *A. planipennis* cuticle that produce its attractive visual signal have been replicated by a process that involves the stamping of a polymer quarter-wave Bragg stack reflector with a set of dies cast from the actual elytra of a female *A. planipennis* (Fig. 2) (14).

Here we report on direct field observations of *A. planipennis* and *A. biguttatus* male behavior toward natural beetle decoys versus three types of synthetic decoys with varying degrees of verisimilitude with respect to the fidelity of bioreplication. These synthetic decoys included: (*i*) a bioreplicated decoy created by a nanomolding process and colored with a polymer functioning as a Bragg reflector; (*ii*) another bioreplicated decoy created by
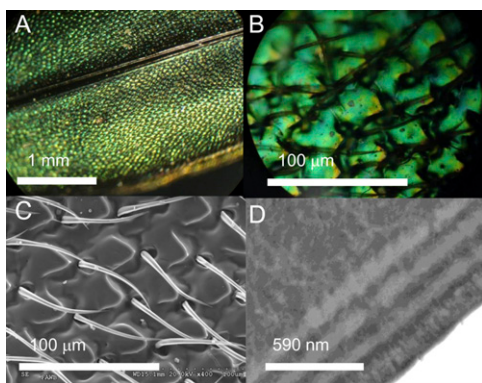

Fig. 1. Structural color and surface topography of *A. planipennis* wings. (*A*) Optical microscopy showing a dorsal view of the beetle elytron. (*B*) Higher-magnification optical microscopy showing spines and cilia. (*C*) Scanning electron micrograph showing a higher-resolution image of the surface topography. (*D*) Transmission electron micrograph of a cross-section of an elytron, showing four alternating layers of differing refractive indices. (*C* and *D* are reprinted with permission from ref. 14.)
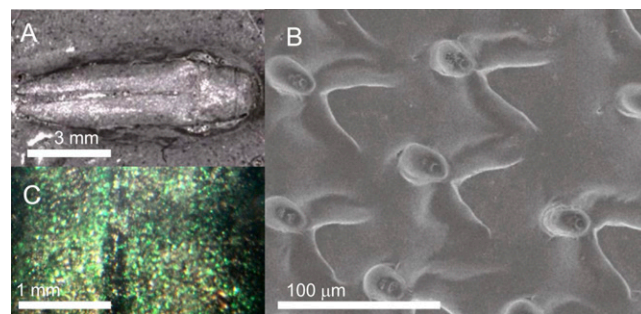
Fig. 2. Nano-bioreplicated decoy characteristics. (*A*) Optical microscopy of the nickel die. (*B*) Scanning electron micrograph of a nickel die used for bioreplication, showing a similar structure as the *A. planipennis* surface (Fig. 1), but without the cilia. (*C*) Optical microscopy of the dorsal view of a nano-bioreplicated *A. planipennis* decoy that reproduces the surface structure of the beetle and is colored by metallic paint. (*A* and *B* are reprinted with permission from ref. 14.)

a nanomolding process and colored with a metallic green paint; and (*iii*) a 3D-printed decoy consisting of a smooth polymer surface without a nanomolded bioreplicated surface structure, also colored with green metallic paint. We investigated whether the nanomolding process could create light-scattering patterns similar to those of real decoys by observing light emissions resulting from the application of a white laser to the surfaces of real and synthetic decoys in a dark room. We hypothesized that a sufficient degree of verisimilitude with respect to color and fine-scale topological features of the elytra could be achieved through the bioreplication process to elicit inflight mating approaches and landings similar to those evoked by real beetles. We also incorporated the bioreplicated decoys into a trapping system in which the electroconductive properties of the decoy are used to electrocute male beetles when they approach and alight on the decoys.

Results

Decoys. Two types of nano-bioreplicated decoys were created that mimicked both the overall shape and fine surface structure details of *A. planipennis* (Figs. 2 and 3*A*). The first type was coated with a Bragg-reflective layer that created structural coloration, whereas the second type was colored with green paint. The painted decoys had been more tightly stamped to the specifications of the nano-imprinted dies created for the replication process, which caused a degradation of the Bragg-reflective layers. These layers were left intact in a lighter stamping procedure used to create the first type of decoy. The same green paint also was applied to 3D-printed decoys, which have the dimensions of a resting female *A. planipennis*, but without replication of fine-scale surface features (Fig. 3*A*).

All three types of fabricated decoys had color spectra similar in peak wavelength to that of *A. planipennis* elytra at 520–540 nm (Fig. 3*B*). Peak intensities of the spectra for all of the fabricated decoys exceeded those of the natural *A. planipennis* and *A. biguttatus* beetle elytra. As expected, the peak reflectance of *A. biguttatus* elytra occurred at a longer wavelength (~610 nm) than that for *A. planipennis*. Despite this difference in base coloration, dead, pinned *A. planipennis* females have been shown to be highly attractive to *A. biguttatus* males (18).

The light-scattering properties of the real beetles and bioreplicated decoys were verified by projection of light from decoys illuminated by a supercontinuum laser (Fig. 4). The back-scattered light from *A. planipennis* beetle elytra comprised conspicuous intense greenish yellow strands (Figs. 4 and 5*A*). Both *A. biguttatus* (Fig. 5*B*) and a nano-bioreplicated decoy (Fig. 5*C*) emitted demonstrable similar strands of greenish light in images created by reflections of the white laser beam. At a distance of 15 cm, all three of these decoys produced textured light patterns including strands
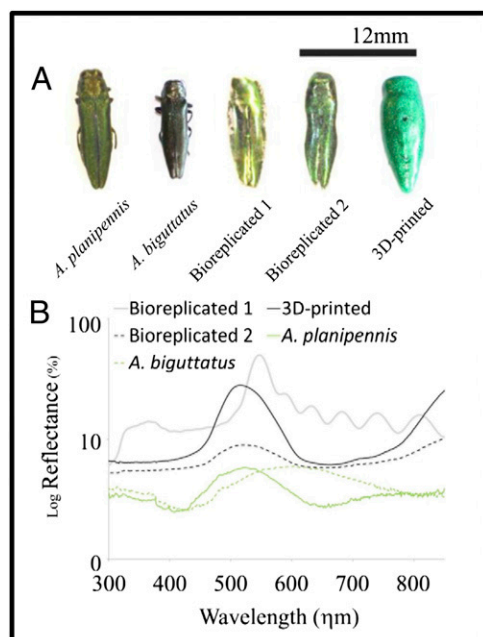
Fig. 3. Natural and fabricated decoys used for attracting buprestid beetles. (*A*) From left to right, an *A. planipennis* female, an *A. biguttatus* female, a nanofabricated decoy constructed by lightly stamping a PET sheet with a Bragg stack reflector over a bioreplicated die (Bioreplicated 1), a nanofabricated decoy constructed by tightly stamping the PET sheet but adding green metallic paint to the underside for more uniform coloration (Bioreplicated 2), and a 3D-printed decoy painted with a green metallic paint (3D-printed). (*B*) Reflectance spectra of each of the decoys as measured by percent reflectance at 1-nm wavelength increments from 300 to 850 nm.

often as narrow as ∼20 mm. Thus, projecting from the cuticle surface, there was <1° of separation between adjacent color bands. In contrast, the unstructured 3D-printed surface produced no noticeable repeated color bands (Fig. 5*D*).

When presented to wild *A. biguttatus* males in the field, all three types of synthetic decoys, as well as dead, pinned *A. planipennis* and *A. biguttatus* female decoys, elicited initial flights by males toward them from ∼0.5 to 1 m away. Furthermore, there were no significant differences in these initially recorded inflight approaches among the decoys (Fig. 6). However, when responding to both species of real females, as well as to both types of bioreplicated decoys, males would nearly always continue to fly toward and alight on them (Fig. 6 and Movie S1). In response to the 3D-printed decoys, male flights were initially directed toward the decoys, but were not completed. Males then either flew off in another direction after coming to within 10–20 cm of the 3D-printed decoys or else would land on the leaf surfaces next to them without touching them (Fig. 6).

We found that copulating male *A. biguttatus* remained mounted on the dead, pinned *A. planipennis* decoys for a mean ± SEM time of 79.0 ± 16.5 s (*n* = 12) and on dead, pinned *A. biguttatus* decoys for 48.5 ± 1.5 s (*n* = 2). None of the synthetic decoys ever elicited a prolonged visitation of more than 2 s. This result was expected, because we did not attempt to replicate the abdominal shape and sexual organs of a female for the synthetic decoys, nor did these decoys have natural coatings of cuticular lipids like the real pinned females. Some of these cuticular lipids have been shown to act as contact sex pheromones in *A. planipennis* (16).

Attraction to Nano-Bioreplicated Decoys on Electrocution Traps. Traps that featured a decoy placed at a 45° angle above the trap opening on a green plastic surface were manufactured. Two steel pins were located at the center of and just below the decoy, creating a 4,000-V potential for electrocution (Fig. 7 and Fig. S1).

Laboratory testing of these traps before field deployment demonstrated that when placed on the traps just below the synthetic decoys, male *A. planipennis* would crawl onto the decoys and be instantly electrocuted, then drop into the receptacle below the decoy. Examination revealed that the beetles were either stunned or killed, with the stunned males remaining that way for more than 15 min. The synthetic decoys proved to be better suited for use in these traps than dead, pinned female beetles because they were better electrical conductors. They could reliably deliver a shock from anywhere on their surfaces, whereas dead beetle decoys required that the males touch both of the pins simultaneously to receive a shock.

In the field, the electroconductive nano-bioreplicated decoys attracted beetles to the traps and captured them via electrical stunning. A movie was obtained confirming that an *A. planipennis* male performed the stereotypical mating flight onto the nano-bioreplicated decoy and subsequently fell into the collection cup (Movie S2). Over the 17-d period in which four of these traps were deployed at the Hungarian oak site as described below, *A. biguttatus* males were caught only during the last 3 d of the experiment, with four specimens captured (Table 1). In an ash plot in Pennsylvania, 16 *A. planipennis* were caught, including two in June when only three traps were running and 14 in the first 11 d of July, when seven traps were deployed. Thus, captures at both sites appeared to increase late in the flight season. Captures of *A. planipennis* were significantly male-biased, exhibiting a 13:3 male:female ratio ($\chi^2 =$ 6.25, df = 1, *P* = 0.012), and the smaller sample of *A. biguttatus* showed a similar trend, with a 3:1 male:female ratio. Several of the specimens of both sexes of either species showed signs of physical damage from electrocution, such as decapitation or distention of the head or reproductive structures. These results suggest that some females had contacted the decoys, despite no previous reports of female *Agrilus* approaching other beetles in nature.

In Hungary, a larger array of nontarget insects was captured in the electrified traps compared with Pennsylvania (Table 1). The Pennsylvania site was easy to access, and so batteries were placed in the traps only when *A. planipennis* was likely to be active, between 0800 and 2000 hours. The Hungarian site was more
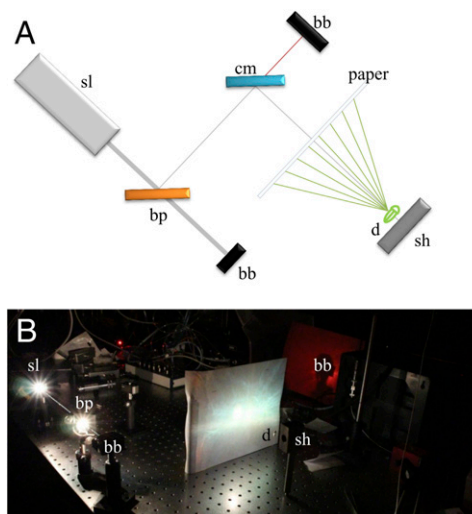

Fig. 4. White-laser scatter projection apparatus for depicting color scattering patterns from real *Agrilus* beetles and synthetic decoys . (*A*) Diagram of the path of a beam generated by the supercontinuum laser (sl), which was directed by a beam pick (bp) and cold mirror (cm) through a hole in the paper onto the illuminated decoy (d) mounted on the specimen holder (sh). Beam blocks (bb) were used as needed to safely contain excess energy not directed to the decoy. (*B*) Actual photo of the apparatus. All of the components are labeled as in the diagram except the cold mirror, which is not visible.
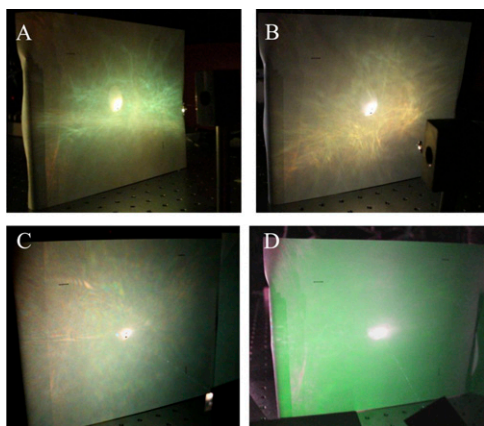
Fig. 5. White laser-generated scattergraphs using different decoys, including *A. planipennis* (*A*), *A. biguttatus* (*B*), a nano-bioreplicated decoy (Bioreplicated 2) (*C*), and a 3D-printed decoy without a bioreplicated surface (*D*).

remote, so batteries were left running continuously and changed at 0900 daily, which allowed for the capture of nontarget insects at dusk and throughout the night until the batteries were usually drained because of a continuous charge resulting from morning dew. The other *Agrilus* species caught consisted almost entirely of *Agrilus angustulus* and *Agrilus obscuricollis,* which are difficult to distinguish from one another. There was no biased sex ratio among these specimens ($\chi^2 = 2.20$, df = 1, $P = 0.138$). These species are known to be highly abundant at this site, being easily observable on the leaves of most oak trees (18). Furthermore, in a previous trapping experiment involving decoy-baited sticky traps, these two species together contributed ~68% of all captures, compared with only 1% of *A. biguttatus* (24). Thus, the finding that 8% of the specimens were *A. biguttatus* in the electrocution traps (Table 1) suggests that these traps may be relatively more effective for *A. biguttatus*. This finding is consistent with previous observations demonstrating that male *A. biguttatus* often landed directly onto decoys, whereas *A. angustulus* usually landed 1–2 cm away on the adjacent surface before approaching the decoy (18).

Finally, 13 beetles from the family Scarabaeidae were caught as well. Five of these were brightly metallic colored specimens of the species *Anomala vitis*. Several of these specimens were found alone with detached wings or legs, which suggested electrocution.

Discussion

The replication of fine-scale surface features of the elytra by nano-bioreplication was critically important for evoking the stereotypical flight approach of the wild males of the *Agrilus* species studied. The heavily stamped nano-bioreplicated type of decoy and the 3D-printed decoys were painted with the same green metallic paint and thus had a similar green base coloration. Midflight during approach, the males apparently recognized the untextured decoys as inauthentic. This in situ behavioral observation is consistent with the observation that the nano-bioreplicated decoys and natural female elytra displayed intense strands of reflected light when illuminated by a white laser (Fig. 5 *A–C*), whereas 3D-printed decoys displayed only a smooth green reflectance (Fig. 5*D*).

Although other studies have demonstrated that the shape of a resting female *A. planipennis* is important for evoking mating responses, there also have been indications of tolerance of a fair amount of deviation from the precise dimensions of a resting female. For example, a pair of detached elytra can attract males if they are affixed parallel to each other on a leaf with the same orientation as a resting beetle (25). Furthermore, a tiger beetle

elytron (17), which very roughly approximates the length and width of resting *Agrilus* beetles of the species studied here, also was found to be capable of evoking male approaches and landings. Thus, all of the decoys used in the present study appear to fall well within the size and shape specifications needed to evoke male attraction responses; indeed, they were all equally capable of eliciting initial attraction by patrolling males. However, wild males approaching the decoys continued to descend and land only on the decoys with real or nano-bioreplicated light-scattering properties.

Because the scattering of light appears to be a crucial factor in promoting male responses, manipulation of the die cast to vary this feature may lead to insight into the physiological capabilities of the *Agrilus* eyes to detect the visual flux of light strands. In turn, further use of the white laser would allow quantification of characteristics of the scattering patterns as needed, at the distances relevant to *Agrilus* behavior.

Although our experiments clearly show that the light-scattering properties of the *Agrilus* cuticle strongly influence the completion of male mating flights, the importance of the bioreplicated structural coloration mechanism is less clear. The spectral emission pattern of the Bragg stack reflector is closer to that of real beetles in having only a single peak in the green portion of the spectrum, whereas the paint used for the other decoys had increasing reflectance in the far-red to IR portions of the spectrum above 800 nm. Although the far-red emissions of the green paint theoretically could have been inhibitory to the *Agrilus* beetles, this was not observed experimentally and otherwise does not seem likely. Specialized receptors dedicated to IR signals exist in specialized organs of pyrophilic buprestids (26), but no such organs are apparent in any *Agrilus* species. Furthermore, 700 nm is approximately the highest wavelength detected in the compound eyes of insects with the best-known discrimination ability of red and far-red signals (27). At the same time, however, the fact that the Bragg stack polymer layers were prone to gradual dissipation in the field, leading to loss of coloration, should be taken into account. Despite these challenges, the Bragg stack colored type 1 decoys performed as well as the type 2, paint-colored decoys.
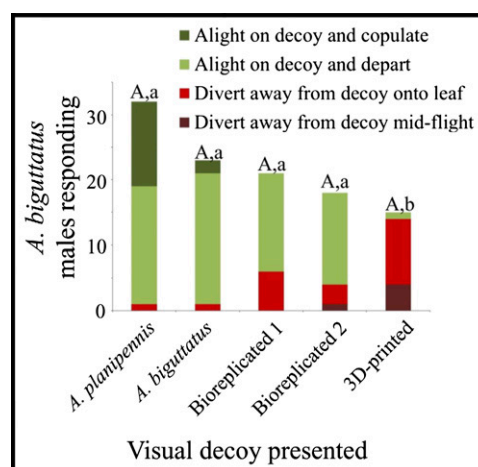

Fig. 6. *A. biguttatus* behavior directed toward each of the five natural and synthetic decoys in a choice experiment, involving $n = 109$ wild males. The frequencies of all positive behaviors were categorized according to the legend. There were no significant differences with respect to the cumulative number of all such approaches to the decoys ($\chi^2 = 7.44$, df = 4, $P = 0.1143$), but there were significant differences among the decoys with respect to flight completion ($\chi^2 = 53.8$, df = 4, $P < 0.0001$), which was calculated as the proportion of observations in the third or fourth category where the decoy was touched by the approaching male (green). Identical letters indicate that the cumulative number of initial approaches (capital) or proportion of flights completed (lowercase) did not significantly differ in Bonferroni-corrected individual comparisons ($\alpha = 0.05$).
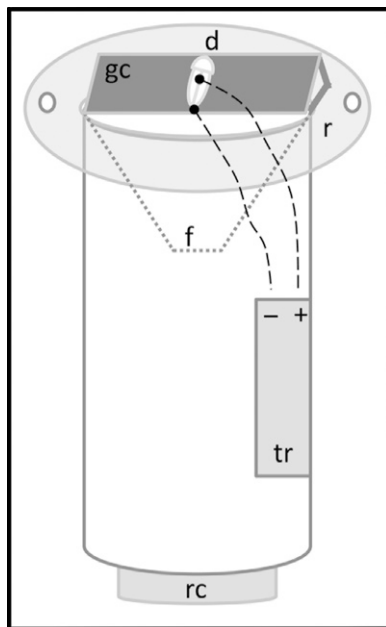
Fig. 7. Electrocution trap components. An *Agrilus* beetle decoy (d) is mounted on a green card (gc) at a 45° angle above the trap opening on its rim (r), which has holes that allow the trap to be hung with rope from tree branches. A funnel (f) extends below into the trapping opening, where a battery-powered transformer (tr) is housed. The transformer is connected with wires (dashed lines) to two steel pins fastened through the center of the decoy and just below it. A removable collection cup (rc) is located at the bottom of the assembly.

Thus, the possibility that the spectral emissions from the Bragg stack polymer are more attractive than the paint, and that improvements to create a more durable bioreplicated decoy with this coating could further improve responses, should not necessarily be ruled out.

The ability to select and nanofabricate the optimal visual signal qualities of a decoy and thus direct male behavior to a specific place on a trap presents opportunities for more refined detection techniques. Already, our ability to electrically stun feral males suggests the realistic possibility of reporting these electrical events via wireless communication to personnel stationed at remote locations. Furthermore, the electrical stunning obviates the use of sticky surfaces to ensnare males, a cumbersome technique that previously had always been used with such decoy-baited traps (24, 25, 28). Sticky surfaces function well for

chemical attractants, such as pheromones, that are not usually negatively affected by accumulation of the trapped insects; however, when a visual decoy is used as an attractant, the sticky surface can quickly become filled with background visual "clutter" from scores of both target and nontarget insects. Such clutter will then have the immediate effect of changing the signal value of the carefully bioreplicated *Agrilus* beetle decoy stimulus. Manipulation of a continually clean visual surface, as offered by our electrified trap, will facilitate continuing efforts to optimize the attractiveness of such decoys and to effectively use them in pest management applications.

Methods

Nano-Bioreplicated and 3D-Printed Decoys. The nano-bioreplication process used for the production of two types of visual decoys has been described elsewhere in detail (14). In brief, a high-fidelity (~200-nm resolution) negative die of nickel was produced from an *A. planipennis* female by physical vapor deposition, followed by electrodeposition of nickel. From this negative die, a positive die of epoxy was produced through successive casting and curing of polymers. Together, the nickel negative die and the epoxy positive die constitute a mold. Next, a quarter-wave Bragg stack reflector comprising alternating layers of poly(vinyl cinnamate) and poly(acrylic acid) was spin-coated on one side of a poly(ethylene terephthalate) (PET) sheet, so that the PET sheet acquired a green color on reflection with a peak at a wavelength of ~540 nm. The other side of the PET sheet was coated with Krylon indoor/outdoor flat black paint to absorb visible light that had not been reflected.

The PET sheet was lightly molded using pressure between the two dies to produce the nano-bioreplicated decoys (labeled "Bioreplicated 1" in Fig. 3A). The light molding preserved the Bragg reflector-produced 540-nm green structural coloration (Fig. 3B) and the fine elytral surface structuring imparted by the molding process was displayed as well. The nano-bioreplicated decoys labeled "Bioreplicated 2" in Fig. 3A were produced by stamping using heavy pressure between the dies, which destroyed the Bragg reflector-produced green color. Here, green coloration was subsequently recovered by painting this type of decoy with Testor's Mystic Emerald spray paint on the underside.

A third type of decoy, labeled "3D-printed" in Fig. 3, was produced by a 3D-printing process performed using a Stratasys Dimension 1200es-SST 3D printer (28). The 3D-printed decoys were made of white acrylonitrile butadiene styrene. A single decoy was printed as 11 discrete layers, each ~0.254 mm thick, and then colored green using the same Testor's Mystic Emerald spray paint used for the Bioreplicated 2 decoys (Fig. 3A).

The visual properties of decoys were characterized in multiple ways. First, reflectance spectra for each decoy were measured using a PerkinElmer Lambda 950 with a 150-mm integrating sphere equipped with a microfocus lens and mechanical iris to establish a beam size of 2 mm. All sample spectra were referenced to a Spectralon reflectance standard.

Finally, a Fianium SC450 supercontinuum laser was used to visualize the light scattering patterns of the decoys in a dark room. This laser produces wavelengths from 450 to 2,400 nm at an average power of 4 W. To prevent damage to the decoy, a beam sampler was used to reduce the power to 1% of the original power, and a cold mirror was used to eliminate any IR light that could damage the decoy. The light from the laser was directed through a 2-mm hole in a sheet

Table 1. Insect captures in electrocution traps baited with nanofabricated decoys to target *A. planipennis* and *A. biguttatus*

Site	Traps with bioreplica (1,2), *n*		Species	Bioreplicated 1	Bioreplicated 2
	June	July			
PA	(1,2)	(3,4)	*A. planipennis*, males/females	4/1	9/2
Hungary	(2,2)	(0,0)	*A. biguttatus*, males/females	2/1	1/0
			Other *Agrilus*, males/females	10/16	12/17
			Other Buprestidae, males/females	1/0	0/0
			Sacarbaeidae, total	7	6
			Diptera (Syrphidae), total	38 (33)	41 (26)
			Others, total	2	7

Between June 8 and June 24 traps were deployed in Hungary to target *A. biguttatus* and in Pennsylvania (PA) to target *A. planipennis*. Between July 1 and July 11, traps were run only at the PA site. The relative numbers of traps (*n*) baited with each decoy type (Bioreplication 1 vs. Bioreplication 2) and the respective insect captures combining both periods for PA are provided.

Domingue et al.

of copy paper onto the specimen (Fig. 4). The specimen was placed 15 cm from the paper, on which 1-cm reference marks were made to allow estimation of the width of color bands projected onto the paper. All real and synthetic beetle decoy types were characterized by laser illumination with the exception of the Bioreplicated 1 decoys. All specimens of this type had degraded and lost their Bragg stack coatings before such characterization was undertaken.

Field Observation Experiment. Field observations of *A. biguttatus* behavior were performed near Mátrafüred, Hungary, in a mixed oak forest where logging activity occurs on an annual basis. In ongoing observational and trapping experiments, *A. biguttatus* has been found along with several other *Agrilus* species. This species tends to congregate on south-facing lower branches of sessile oak trees, *Quercus petraea* (Matt.) Liebl., which are located within 10m of cut log piles. Observations were made on such trees on June 10–19, 2013, during sunny periods between 1130 and 1500 hours.

Five decoys were pinned to the leaves including, a real female *A. planipennis*, a real female *A. biguttatus*, and three synthetic decoys (Bioreplicated 1, Bioreplicated 2, and 3D-printed) (Fig. 2A). To assess and compare visual attraction to the five models, they were placed on different neighboring leaves, ~10 cm apart, and observed for 10-min periods. A bare pin was also deployed alongside the decoys, which was never approached. Between observation periods, the specimens were rearranged such that positional biases would not develop. In addition, the entire array of decoys was replaced daily. A total of 109 approaches were noted over the course of 19 of these 10-min periods, on six different days. Behaviors noted included (*i*) initial approach toward a decoy, (*ii*) landing on a decoy or flying away without landing, and (*iii*) time spent on a decoy after landing on it. Contacts of >2 s indicate the initiation of copulation (18).

Electrocution Traps. Traps were constructed using 10-cm PVC piping as a collection device and platform for two 9- $\times$ 13- cm^2 green plastic cards (Fig. 7 and Fig. S1), similar to those used in previous *Agrilus* trapping applications (24). The card on one side was positioned over a funnel in the center of the piping, such that beetles electrocuted from its surface would fall downward into the funnel and trap below. A bioreplicated decoy was placed on the surface of this card, with one steel pin located just below it and another steel pin through its middle. These pins were electrically connected to a transformer providing a 4,000-V potential using two C batteries. The transformer was derived from a battery-operated electric fly swatter (BugKwikZap). The lower pin was permanently connected to the card, whereas the upper pin was removable, connected to the circuit by an alligator clip, which allowed for replacement of the decoy when desired. Kill strips (Vaportape II; Hercon Environmental) were placed inside the detachable cup of each trap to prevent stunned insects from possibly crawling or flying up and out of the trap.

Four of the traps were run in the Hungarian site described above between June 8 and June 24, and three other traps were run concurrently in an isolated plot of ash trees on the University Park campus of Pennsylvania State University consisting of ~2,000 white ash trees (*Fraxinus americana*) that were heavily infested with *A. planipennis*, as evidenced by observations of crown dieback, exit holes, and readily observable flying adults. This site was surrounded by mixed agricultural, residential, and academic landscapes. The four traps in Hungary used two Bioreplicated 1 decoys and two Bioreplicated 2 decoys. The three traps used in Pennsylvania initially included one Bioreplicated 1 decoy and two Bioreplicated 2 decoys. Between July 1 and July 11, the experiment was terminated in Hungary, and all seven traps were run at the PA site, with three Bioreplicated 1 decoys and four Bioreplicated 2 decoys. All traps were baited with (Z)-3-hexen-1-ol, a green leaf volatile that has been shown to increase *A. planipennis* trap captures on sticky prism traps (29). (Z)-3-hexen-1-ol dispensers were provided as premade plastic packets (ChemTica Internacional), which had been measured to release 25 mg per day for 45 d by measuring weight loss at room temperature (22 °C).

Statistical Analyses. For comparing the choices made by the field population of *A. biguttatus*, a log-linear model was fit to the data using the Proc CATMOD feature of SAS version 9.2. This model allowed comparison of the proportion of males flying toward each decoy. The proportion of complete vs. incomplete mating flights was compared among the five decoys using Fisher's exact test. All possible individual comparisons were made between decoy types for flight completion and were Bonferroni-corrected. For the electrocution traps, simple χ^2 comparisons were made with reference to expectations of a balanced sex ratio and preference between the two nanofabricated decoys. Because the Pennsylvania experiments deployed more of the type 2 nano-bioreplicated decoys than type 1 decoys on the traps, the expectations were weighted accordingly.

1. Xu J, Guo Z (2013) Biomimetic photonic materials with tunable structural colors. *J Colloid Interface Sci* 406:1–17.
2. Dushkina N, Lakhtakia A (2013) Structural colors. *Engineered Biomimicry*, eds Lakhtakia A, Martín-Palma RJ (Elsevier, Waltham, MA), pp 267–303.
3. Arikawa K (2012) Color sensors of butterflies. *Frontiers in Sensing: From Biology to Engineering*, eds Barth FG, Humphrey JAC, Srinivasan MV (Springer, New York), pp 43–55.
4. Ng R, Zang R, Yang KK, Liua N, Yang S-T (2012) Three-dimensional fibrous scaffolds with microstructures and nanotextures for tissue engineering. *RSC Adv* 2:10110–10124.
5. López-Bosque MJ, et al. (2013) Fabrication of hierarchical micro-nanotopographies for cell attachment studies. *Nanotechnology* 24(25):255305.
6. Lee TR, et al. (2013) On the near-wall accumulation of injectable particles in the microcirculation: Smaller is not better. *Sci Rep* 3:2079.
7. Moolman MC, Huang Z, Krishnan ST, Kerssemakers JWJ, Dekker NH (2013) Electron beam fabrication of a microfluidic device for studying submicron-scale bacteria. *J Nanobiotechnology* 11:12.
8. Marsh D, Kennedy JS, Ludlow AR (1978) Analysis of anemotactic zigzagging flight in male moths stimulated by pheromone. *Physiol Entomol* 3:221–240.
9. Blum MS (1969) Alarm pheromones. *Annu Rev Entomol* 14:57–80.
10. Matsumura F, Coppel HC, Tai A (1968) Isolation and identification of termite trail-following pheromone. *Nature* 219(5157):963–964.
11. Boeckh J (1962) Elektrophysiologische untersuchungen an einzelnen geruchsrezeptoren auf den antennen des totengräbers (Necrophorus, Coleoptera). *J Comp Physiol* 46:212–248. German.
12. Hansson BS, Ljungberg H, Hallberg E, Löfstedt C (1992) Functional specialization of olfactory glomeruli in a moth. *Science* 256(5061):1313–1315.
13. Witzgall P, Kirsch P, Cork A (2010) Sex pheromones and their impact on pest management. *J Chem Ecol* 36(1):80–100.
14. Pulsifer DP, et al. (2013) Fabrication of polymeric visual decoys for the male emerald ash borer (*Agrilus planipennis*). *J Bionics Eng* 10:129–138.
15. Lelito JP, et al. (2007) Visually mediated "paratrooper copulations" in the mating behavior of *Agrilus planipennis* (Coleoptera: Buprestidae), a highly destructive invasive pest of North American ash trees. *J Insect Behav* 20:537–552.
16. Lelito JP, et al. (2009) Behavioral evidence for a contact sex pheromone component of the emerald ash borer, *Agrilus planipennis* Fairmaire. *J Chem Ecol* 35(1):104–110.
17. Lelito JP, et al. (2011) Field investigations of the mating behaviors of *Agrilus cyanescens* and *Agrilus subcinctus*. *Can Entomol* 143:370–379.
18. Domingue MJ, et al. (2011) Field observations of visual attraction of three European oak buprestid beetles toward conspecific and heterospecific models. *Entomol Exp Appl* 140:112–121.
19. Moraal LG, Hilszczanski J (2000) The oak buprestid beetle, *Agrilus biguttatus* (F.) (Coleoptera: Buprestidae), a recent factor in oak decline in Europe. *J Pest Sci* 73:134–138.
20. Schlag MG (1992) Oak decline in Europe and its causes as seen from a phytopathological point of view. *Cent.bl. gesamte Forstwes* 111:243–266.
21. McManus M, Csóka G (2007) History and impact of gypsy moth in North America and comparison to the recent outbreaks in Europe. *Acta Silv. Lignaria Hung.* 3:47–64.
22. Durrer H, Villiger W (1972) Schillerfarben von *Euchroma gigantea* (L.): (Coleoptera: Buprestidae): Elektronenmikroskopische untersuchung der elytra. *Int J Insect Morphol* 1:233–240. German.
23. Schultz TD, Rankin MA (1985) Developmental changes in the interference reflectors and colorations of tiger beetles (*Cicindela*). *J Exp Biol* 117:111–118.
24. Domingue MJ, et al. (2013) Field trapping of European oak buprestid beetles using visual and olfactory cues. *Entomol Exp Appl* 148:116–129.
25. Domingue MJ, et al. (2013) Visual and chemical cues affecting the detection rate of the emerald ash borer in sticky traps. *J Appl Entomol* 137:77–87.
26. Vondran T, Apel KH, Schmitz H (1995) The infrared receptor of *Melanophila acuminata* De Geer (Coleoptera: Buprestidae): Ultrastructural study of a unique insect thermoreceptor and its possible descent from a hair mechanoreceptor. *Tissue Cell* 27(6):645–658.
27. Qiu X, Arikawa K (2003) Polymorphism of red receptors: Sensitivity spectra of proximal photoreceptors in the small white butterfly *Pieris rapae crucivora*. *J Exp Biol* 206(Pt 16):2787–2793.
28. Domingue MJ, et al. (2014) Detecting emerald ash borers (*Agrilus planipennis*) using branch traps baited with 3D-printed beetle decoys. *J Pest Sci*, 10.1007/s10340-014-0598-y.
29. Grant GG, Ryall KL, Lyons DB, Abou-Zaid MM (2010) Differential response of male and female emerald ash borers (Col., Buprestidae) to (Z)-3-hexenol and manuka oil. *J Appl Entomol* 134:26–33.